AD_____
(Leave blank)

Award Number:
W81XWH-07-1-0035

TITLE:
The Aged Microenvironment Influences Prostate Carcinogenesis

PRINCIPAL INVESTIGATOR: Daniella Bianchi-Frias

CONTRACTING ORGANIZATION:
Fred Hutchinson Cancer Research Center
Seattle, WA 98109

REPORT DATE:
December 2008

TYPE OF REPORT:
Annual Summary

PREPARED FOR: U.S. Army Medical Research and Materiel Command
Fort Detrick, Maryland 21702-5012

DISTRIBUTION STATEMENT: (Check one)

× Approved for public release; distribution unlimited

□ Distribution limited to U.S. Government agencies only; report contains proprietary information

The views, opinions and/or findings contained in this report are those of the author(s) and should not be construed as an official Department of the Army position, policy or decision unless so designated by other documentation.

REPORT DOCUMENTATION PAGE

Form Approved
OMB No. 0704-0188

1. REPORT DATE *(DD-MM-YYYY)*	**2. REPORT TYPE**	**3. DATES COVERED** *(From - To)*
31/12/08	Annual Summary	01 DEC 2007 - 30 NOV 2008

4. TITLE AND SUBTITLE

The Aged Microenvironment Influences Prostate Carcinogenesis

5a. CONTRACT NUMBER
W81XWH-07-1-0035

5b. GRANT NUMBER
PC060754

5c. PROGRAM ELEMENT NUMBER

6. AUTHOR(S)

Daniella Bianchi-Frias

5d. PROJECT NUMBER

5e. TASK NUMBER

5f. WORK UNIT NUMBER

7. PERFORMING ORGANIZATION NAME(S) AND ADDRESS(ES)

Fred Hutchinson Cancer Research Center
1100 Fairview Avenue North
P.O. Box 19024
Seattle, WA 98109

Email: gmail@fhcrc.org

8. PERFORMING ORGANIZATION REPORT NUMBER

9. SPONSORING / MONITORING AGENCY NAME(S) AND ADDRESS(ES)

U.S. Army Medical Research
And Materiel Command
Fort Detrick, MD 21702-5012

10. SPONSOR/MONITOR'S ACRONYM(S)

11. SPONSOR/MONITOR'S REPORT NUMBER(S)

12. DISTRIBUTION / AVAILABILITY STATEMENT
Approved for public release; distribution unlimited

13. SUPPLEMENTARY NOTES

14. ABSTRACT The greatest factor for the development of prostate adenocarcinoma is advanced age. Emerging evidence suggests that molecular alterations in the aged prostate microenvironment mediated by stromal aging and senescence are key factors regulating carcinogenesis and neoplastic progression. We used normal mouse prostate epithelial and adjacent stromal cells microdissected *in situ* from young and old animals, to identify factors altered by the aged stroma that may place the prostate gland at risk for developing prostate cancer. Expression profiling demonstrated clear differences in gene expression between old and young prostate stroma, with 63 genes exhibiting significant transcript abundance levels given a moderate estimate of false positive differences of 10%. Genes associated with inflammation, oxidative stress, and structural proteins were among the genes most substantially altered with aging. Factors identified in this study, such as ApoD and Ccl8, were selectively expressed and up-regulated only in the aged prostate stroma and not in the prostatic epithelium or inflammatory cells. The aged prostate microenvironment was characterized by a pro-inflammatory gene expression profile and the presence of high numbers of inflammatory cells. Additionally, structural alterations were observed in the aged prostate. Fluorescence and ultrastructural microscopic analysis revealed a collagen matrix network significantly disrupted in the aged prostate. It is plausible that both the alteration in the collagenous stroma and the infiltration of inflammatory cells are likely to be acting in concert with one another to produce fundamental changes in both the prostate epithelial and stromal cells that can lead to prostate tumorigenesis and/or progression. We propose that these changes contribute in a coordinated way to induce and/or sustain prostate tumorigenesis- on one hand by altering the extracellular matrix and, on the other, signaling through the NK-kB pathway for immune infiltration. Taken together, these observations may aid in a better understanding of the causative role of aging in human prostate cancer development and progression

15. SUBJECT TERMS
Microarray, aging, microenvironment, prostate

16. SECURITY CLASSIFICATION OF:			**17. LIMITATION OF ABSTRACT**	**18. NUMBER OF PAGES**	**19a. NAME OF RESPONSIBLE PERSON**
a. REPORT	**b. ABSTRACT**	**c. THIS PAGE**			Daniella Bianchi-Frias
U	U		UU	24	**19b. TELEPHONE NUMBER** *(include area code)*

Table of Contents

Page

INTRODUCTION:

The greatest single risk factor for the development of prostate adenocarcinoma is advanced age [1-5]. Emerging evidence suggests that molecular alterations in the aged prostate microenvironment mediated by stromal aging and senescence are key factors regulating carcinogenesis and neoplastic progression [6,7]. However, no functional studies have been reported that definitively provide mechanistic evidence of cause and effect. This proposal is designed to investigate the role of the aged-stroma microenvironment in prostate carcinogenesis. Our *hypothesis is that gene expression differences can be identified between normal stroma from young vs. old mice, and that candidate genes identified in the aged-stroma have the potential to influence the proliferation, survival, or invasive capabilities of adjacent transformed epithelium via paracrine mechanisms.* The ultimate goal of this proposal is to provide strong preclinical data that can be translated into novel human studies of prostate cancer prevention.

BODY:

Comparative histological analysis of the mouse prostate gland from young and old animals. Mouse prostate glands from 4- and 24-months old C57BL/6 mice were stain with hematoxylin and eosin for histological studies. Overall, each prostate lobe showed subtle differences in morphology with aging (Figure 1). Focal atrophy of a small number of acini as well as epithelial atypia coexisted with morphologically normal acini. The stromal layer adjacent to the epithelial cells was generally more disorganized in old animals than in young animals with little evidence of cell orientation (arrowhead). Interestingly, we found a higher number of inflammatory cell foci with their characteristic small size and little cytoplasm in the aged prostates compared to young prostates (Figure 1, arrows).

By double immunofluorescent staining for smooth-muscle cells (anti-smooth-muscle-actin) and fibroblast (anti-vimentin), we determined that 95% of the adjacent stromal cells stained positive for smooth-muscle actin and only 5% stained positive for vimentin (Figure 2). Thus, the majority of the adjacent cellular stroma is represented by smooth muscle cells and few fibroblasts. The latter finding is of importance inasmuch as the stromal population targeted for capture in the current study may be similarly comprised of smooth muscle cells and few fibroblasts.

Since the focus of this study was to identify age related stromal factors that could potentially altered the behavior of the luminal epithelial cell, we laser captured microdissected the smooth-muscle/ fibroblastic layer surrounding the epithelial cells, thus avoiding any endothelial or inflammatory cells that could be present in the interductal stroma.

Laser captured microdissection can be use to analyze the gene expression patterns in the aged stroma. Sample purity: A key component of our experimental design centered on the analysis of aging-related changes in the stromal compartment of the prostate isolated from its *in situ* environment. Thus, an approach for acquiring pure stromal populations with minimal epithelial cell contamination was essential. We performed a pilot study where we laser capture microdissected the prostatic adjacent stroma (surrounding the epithelial cells) and the luminal epithelial cells from five young (4 months-old) and five old (20 months-old) mice. The RNA was extracted and hybridized to a customized mouse prostate cDNA array (MPEDB array). Gene expression analysis (Log2 Ratios) demonstrated that stromal and epithelial markers were highly expressed in the stroma and epithelial samples respectively (Figure 3B). To further characterize the relationships between the two cell-type compartments and between age groups, we

performed Principal Component Analysis (PCA) for all the genes in the arrays (Figure 3A). PCA clearly identified a subset of genes that discriminated between epithelial and stroma samples, suggesting that the major differences between samples (53% of the total variance) resulted from the differential expression of large numbers of genes between the stroma and epithelial compartments. All together, these results demonstrate that highly enriched population of stroma cells can be captured by microdissection.

Aged-related changes in gene expression in the mouse prostate stroma microenvironment: We performed gene expression profiling using RNA isolated from micro-dissected benign mouse prostate stroma from young (n=5; aged 4 months) and old (n=5; aged 24 months) wild-type C57BL/6 mice. RNA was amplified and hybridized to a customized mouse prostate-specific cDNA microarray containing ~8,300 genes (MPEDB array). Thirty nine genes exhibited significant alterations based on a Student T-test analysis ($p< 0.005$). However, when multiple testing correction was apply, only ten genes were significantly altered given a moderate estimate of false positive differences of 10% based on SAM procedure. Therefore, in order to expand the list of significant altered genes, we performed an additional microarray experiment from LCM stroma from a new set of young (n=12; 4-months old) and old (n=12; 24-months old) mice and used a microarray platform containing ~ 40.000 genes (customized Agilent 44K whole mouse genome oligonucleotide microarray; Figure 4). Using the Agilent arrays, we identified that sixty three genes exhibited significant age-related changes based on SAM procedure (FDR<10%) applying a two-sample unpaired t-test (for a complete list of the 63 genes, see Table 1). A number of genes known to be associated with *in vivo* aging and/or *in vitro* senescence in other tissues and species were confirmed by the current study. Within the up-regulated genes (n=59), 15 (10%) encode proteins that could be linked to an inflammatory/immune response including Ccl5, Ccl7, Ccl8 and Il7R, suggesting that the aged prostate presents a pro-inflammatory environment. Interestingly, it has recently been shown that the expression of CCL8 in endometrial stromal fibroblast is regulated by paracrine factors secreted by leukocytes[8], this finding suggests that the aged smooth-muscle/fibroblastic stroma may be responding to factors secreted by inflammatory infiltrates in the aged prostate. Additionally, the gene expression profile demonstrated an increased expression of genes involve in oxidative stress response and known to be altered in prostate cancer, including ApoD and Serpinb5 (Maspin). Our findings regarding alterations of ApoD expression with aging and senescence, is supported by previous reports demonstrating an increase of ApoD transcript levels in the brain of old mice and post-mortem human subjects (68±83-year-old) as well as in cultured cells as a response to inflammation and senescent inducers [9-13].

Taken together, it is likely that cumulative environmental stress (e.g., oxidative damage and aged-related alteration of the collagen matrix) associated with the normal process of aging may evoke an inflammatory response which in turn may influence prostate carcinogenesis in the elderly.

Quantitative RT-PCR confirmed the up-regulation of Ccl8 and ApoD in the aged LCM stroma (Figure 5A and 5B). ApoD and Ccl8 were found to be primarily expressed in the stroma since their transcript levels in LCM epithelium were much lower compared to the stroma samples and no differences were observed between young and old epithelium. This observation strongly suggests that prostate tissue aging is not homogeneous in nature, in that each cell type is responding to aging differentially, at least at the molecular level. Additionally, we found that up-

regulation of APOD and CCL8 also correlates with *in vitro* senescence of human prostate fibroblast (Figure 5C).

Biological pathway analysis of the aged prostate stroma expression profiles. We used Gene Set Enrichment Analysis (GSEA) to evaluate whether stromal aging was associated with enrichment for specific pathways. For that, we used Gene Ontology gene sets (C5) and the curate gene sets (C2), the later gene set included a senescence-associated gene list generated from our human prostate senescent profile. One-hundred and sixty four GO gene sets (C5) were found to be significantly enriched in the aged stroma. As predicted, a significant enrichment of up-regulated genes implicated in inflammatory response and Cytokine/Chemokine activity were observed. Additionally, up-regulated genes involved in the NF-κB cascade were also enriched in the aged stroma, consistent with recent reports suggesting a role of the NF-κB transcription factor signaling in mammalian aging [14-16]. For the down-regulated genes, collagen binding and pro-collagen genes were significantly enriched, in accordance to our observation that pro-collagen genes are down-regulated with aging.

When the curate data sets were analyzed (C2), we found 661 and 9 pathways that were significantly represented in our up-regulated and down-regulated aged stroma gene list, respectively. Among the gene sets, aging related profiles from mouse aged neocortex, cerebellum, hippocampus and kidney were enriched as well as the senescent associated gene list identified previously in our laboratory. These results suggest that the molecular phenotype of aging is somehow common between different organs and that a correlation between *in vivo* aging of the mouse prostate stroma and *in vitro* senescence of human prostate fibroblast exist.

Inflammation in the aged prostate. The aging-associated transcriptional profile suggests that the aged prostate presents a pro-inflammatory environment with the induction of pro-inflammatory chemokines. To demonstrate that the aged-associated gene expression profile obtained from microdissected adjacent stroma is intrinsic to the aging of the smooth muscle cells and not a reflection of an increased number of inflammatory cells in the aged prostate stroma samples, we then compared the stromal gene expression profile with that obtained from a population of white blood cells isolated from young and old C57BL/6 mice (Figure 6). Gene expression comparison between stroma, epithelial and white blood cells samples clearly demonstrated that a number of genes shown to be overexpressed in the aged stroma are indeed primarily expressed in the stroma compartment and not in white blood cells or epithelial cells (Figure 6, asterisk). These results proved that the aging stromal profile is indeed intrinsic to the smooth-muscle/fibroblastic adjacent stroma and not due to an increase number of inflammatory cells in the microdissected aged stroma.

Given that our expression profile analysis suggests that the age prostate present a pro-inflammatory environment, we then wanted to determine the composition of the immune cell population in the mouse prostate. By immunohistochemistry stain for immune cells, we were able to demonstrate an increased in T-cell, B-cell and to a lesser extent macrophages in the aged prostate (Figure 7). T-cells and macrophages were not only present in cluster foci in the interglandular stroma but also infiltrating into the smooth-muscle/fibroblastic stroma as well in the luminal epithelium.

The presence and increment of these immune cells in the aged tissue prompted us to investigate the potential reasons for the infiltration of these immune cells. By H&E staining, we were able to discard the possibility of an inflammatory response due to bacteria infection, since

neither obvious bacteria infection nor the associated neutrophilic infiltrates were present in the mouse prostate. Therefore, the increased inflammatory state observed in the aged prostates may be explained by several factors: a) increase levels of chemoattractants from the aged smooth-muscle fibroblastic stroma, such as Ccl8, Ccl5, possibly via NF-kB pathway; b) a disrupted collagenous matrix that promotes an inflammatory state and/or c) a decrease in testosterone levels which has been associated with increased levels of inflammatory cytokines and prostate tissue infiltration. Taken together, we believe that genetic and epigenetic factors might have been acting in concert to cause the immune up-regulation observed in the aged prostate.

Although, conflicting data exist regarding the causal effect of chronic inflammation with prostate cancer, there is a significant volume of compelling evidence supporting a role for inflammation in the pathogenesis of prostate cancer [17]. Thus, our observation demonstrating an increased in inflammation in the prostate from aged animals, suggests that aging correlates with a pro-inflammatory state which in turn may well influence prostate neoplasia.

An additional interesting observation was a dramatic increased in autoantibodies (IgM and IgG) in the aged prostate (Figure 7B). What are these autoantibodies recognizing in the aged tissue is still unknown, one possibility is that the aged/senescent cells are secreting senescence-antigens that will bind these IgM and IgG autoantibodies for its recognition and degradation[18,19].

Extracellular matrix alterations in the aged prostate. We only observed 4 genes down-regulated with aging in the mouse prostate stroma considering an FDR <10% (Table 1). However, when a less stringent criteria is apply ($p<0.05$) we found several genes encoding structural proteins to be down-regulated with aging. Transcripts encoding extracellular matrix components for Type I, Type III and Type IV collagen were among the genes most substantially altered with aging and their downregulation was validated by qRT-PCR (Figure 8A). Similar observations have been reported *in vivo* in both humans and mice[20,21] and in senescent cell *in vitro* [18].

Collagen structure in vivo. Comparison of young and old prostate. A series of related fluorescence and ultrastructural microscopic analysis were performed to determine the relationship between collagen structure and aging. Examination of the ECM surrounding prostate epithelial cells by immunofluorescent staining for Collagen Type I and picrosirius red (a selective staining agent for collagen) demonstrated that the majority of the stroma around the prostatic ductal structure is fibrillar collagen (Figure 8C and 8D). Interestingly, although immunofluorescence detection for Type-I collagen did not show substantial differences at the protein level between young and old prostate tissue, it revealed a disorganized collagen matrix network with a coarse appearance and less regular distribution of the collagen fibers in prostates from old animals compared to the fine collagen fibers and highly organized network in prostates from young animals (Figure 8A and 8B, respectively). Thirty micrometers sections from anterior prostate from young and old mice were stain with Collagen Type I and evaluated by confocal microscopy. A stack of images inside the intact tissue were collected and analyzed for collagen fiber organization. Analyses of these images confirmed the collagen fibers alterations observed in the 7 μm thin sections, demonstrating that the alterations in the collagen fibers are not due to mechanical damaging from sectioning. Six scoring criteria were used to quantify the differences (organize, compact, sharp, disorganized, swollen and fuzzy collagen fibers). We found that collagen fiber appearance was significantly different between young and old prostate, demonstrating that >70% of old prostate have a disorganized, swollen and fuzzy fibers ($p<0.05$) compared to the organized, compact and sharp collagen fiber appearance from young mice

($p<0.005$) (Figure 8B). Similar alterations were observed in sections from the dorsal, lateral and ventral lobes, however to quantify the observations, the wider stroma layer in the anterior lobe was chosen to facilitate the scoring.

Since little is known about the involvement and function of collagen matrix organization, and density in prostate cancer, we wanted to investigate in greater detail the structural alterations of the collagen network surrounding normal aged epithelium from intact tissue. To visualize the three-dimensional organization of the collagenous stroma, scanning electron microscopy using prostates from young and old animals treated with serial washes of 10% NaHO solution to remove all cellular elements was performed [22,23]. The acellular preparations showed that a smooth and grossly homogeneous fibrous sheet lines the inner layer of the prostatic ducts which directly faces the empty acinar space. On the outside of the ducts, a spongy-like organization was revealed and demonstrated that in the young prostate a meshwork of loosely woven fibrils is present with an intact structure of distinct collagen bundles while in aged mice collagen bundles were adhere to each other (Figure 8C). These observations are in a fashion similar to that seen by the immunofluorescent staining for Collagen Type I (Figure 8B). Taken together, these results suggest that the collagenous stroma in aged mouse prostate is characterized by a disorganized and disrupted collagen matrix. To our knowledge, this is the first study that demonstrates alterations in the collagen network with aging in prostate tissue.

To further characterize the structural organization of the collagen fibers and the organization and orientation of the cellular components in the aged mouse prostate, transmission electron microscopy (TEM) was performed. Although contradictory, we found that even when the aged animals had the lowest levels of procollagen I alpha-1 mRNA they presented the greatest amount of collagen fibers in the stroma as detected by TEM (Figure 9). Furthermore, although the basement membrane did not present any obvious disruptions with aging, epithelial cytoplasmic projections were observed extending towards the extracellular matrix in the aged prostate, indicating that the basement membrane is somehow allowing these epithelial cells to reach into the extracellular matrix. At the cellular level, in aged prostates the smooth muscle cells presented a less clear orientation within the stroma and did not have a continuous parallel arrangement as observed in young prostate. In agreement with these results, similar ultrastructural phenotypes have recently been observed in the aged Mongolian gerbil ventral prostate[24].

Increasing amount of evidences support the potential implications of the collagen content, fiber structure, and organization as key determinants of tumor cell behavior [25-28]. Thus, the structural changes observed in the aged prostate may plausible be involved in prostate tumor formation and progression.

Correlation between mouse *in vivo* aging stroma and human *in vitro* senescence. To begin to address the relevance of factors identified in the aged murine prostate stroma with human senescence transcriptional signatures, RT-PCR was performed for genes encoding soluble factors that have been shown to be up-regulated with *in vitro* senescence such as Areg, Cxcl12, Hgf, IL-6, IL1a, Ctgf, Gm-csf, among others [6,29,30]. Unexpectedly, none of the candidate factors were up-regulated in the aged mouse prostate stroma. However, as described above, transcripts that were found to be up-regulated in the aged stroma, such as ApoD and Ccl8 were significantly higher in human prostate senescent fibroblast when compared to pre-senescent fibroblast (Figure 5C).

For a more global approach, the transcriptional profile of aged murine stroma, identified in this study, was compared with previously identified transcriptional profiles of human prostate senescent fibroblasts, induce to senesce by different means (H_2O_2, Bleomycin, replicative senescence and overexpression of p16 and oncogenic RAS ([6] and data not publish from our laboratory). Out of 264 genes significantly altered in mouse aged stroma (FRD<25%), 37 genes were also significantly altered with senescence in at least one senescent inducer (Figure 10). Genes involved in the NF-kB pathway, such as Stat1 and Tlr1; cell proliferation / apoptosis, such as IER3; EHF; LRPAP1 and inflammation such as CCL7; CXCL16; B2M; IL7R were among the genes whose expression was modify in both *in vivo* aging and *in vitro* senescence. The alteration of these gene groups are in agreement with the Biological functions identify in the GSEA analysis as describe below.

In order to determine if the aged prostate presents an increase number of senescent cells, Senescent-Associated ß-Galactosidase staining (SA-b-Gal) was performed in young and old prostate. We did not find any stroma cells positive for SA-b-gal, however, we noticed SA-b-gal positive epithelial cells but no differences between young and old prostate were observed. In addition to the SA-b-gal staining, we tried other *in vivo* senescent markers such as gamma-H2AX and we did not find any increase number of cells with H2AX foci. We have also performed IHC staining for 53BP1 and p16 with no success. Although several studies have demonstrated that senescent cell accumulate with aging [31-34], the lack of an increase in senescent cells, based on SA-B gal stain, has also been reported in other tissues from aged mice [35]. Thus, senescent cells may not accumulate in the aged prostate or they may arise in the prostate but are clear out by an unknown mechanism, possibly through macrophages or Natural killer cells. The dramatic increased in autoantibodies (IgM and IgG) in the aged prostate, identified in the current study, may rise the question of whether aged/senescent cells are secreting senescence- antigens that will bind these IgM and IgG autoantibodies for its recognition and degradation. Recent studies have give clues to this idea [18,19].

Taken together, these results suggest that the stroma cells in the aged mouse prostate cannot be consider senescent, and that they are of a different phenotype. Nevertheless, as mentioned above, qRT-PCR revealed that several genes found in this study to be up-regulated with *in vivo* aging were also up-regulated in human prostate senescent fibroblast. Thus, these observations may indicate that only subsets of molecules are commonly activated during *in vivo* aging and *in vitro* senescence.

KEY RESEARCH ACCOMPLISHMENT:

- We have demonstrated that laser capture microdissection technique can be use to obtain highly enriched population of prostatic stromal cells.
- We have identified an age-associated gene expression profile of the mouse prostate stroma isolated from its *in situ* environment.
- We have confirmed that factors identify in this study, such as ApoD and Ccl8, were selectively expressed and up-regulated only in the aged prostate stroma and not in the prostatic epithelium or inflammatory cells. Additionally, we have shown that these factors were altered both in *in vivo* aged stroma and *in vitro* human senescent cells.
- We have demonstrated that the extracellular collagenous stroma in aged prostate presents a disorganized and disrupted collagen matrix.

- We have demonstrated that the prostate microenvironment from aged mice is characterized by a pro-inflammatory state with a high number of inflammatory cells.
- We have demonstrated that the molecular phenotype of *in vivo* aged stroma does not correlate with the senescence-associated secretory phenotype (SASP) of *in vitro* senescent fibroblast.

REPORTABLE OUTCOMES:

Poster presentation:

Poster title: "The Aged Prostate Microenvironment: Implications for Prostate Carcinogenesis" Presented at the MCB Graduate Student Reception / Human Biology Division. FHCRC. September 12th, 2008. Seattle, WA.

Talks:

"Influence of the Aged Microenvironment on Prostate Carcinogenesis". Friday Night Seminar. FHCRC. June 27, 2008. Seattle, WA.

"Influence of the Aged/Senescent Microenvironment on Prostate Carcinogenesis". Human Biology Retreat. FHCRC. March 31-April 1st, 2008. Semiahmoo Resort, WA.

Manuscripts in preparation:

1. **Daniella Bianchi-Frias**, Funda Vakar-Lopez, Ilsa M Coleman, May Reed, Steven S Plymate, and Peter S. Nelson. Molecular and Phenotypic Characterization of the Aging Murine Prostate Microenvironment: Implications for Carcinogenesis. (in progress)

2. Damodarasamy M, Karres N, Chang CT, **Bianchi-Frias D**, Vernon RB, Reed MJ. The effect of age on the structural and functional characteristics of murine 3D collagen. (in progress)

CONCLUSION:

In this study, we have made five main observations: First, aging-related changes in gene expression exist in the mouse prostate and that these changes are cell-type specific. Second, the molecular phenotype of the aged prostate stroma is characterized by the over expression of factors involved in oxidative/environmental stress response and inflammation. Third, a pro-inflammatory state exists in the aged prostate with an increased in inflammatory infiltrates. Fourth, the collagen matrix network is significantly disrupted in the aged prostate. And five, that the aged stroma cannot be consider senescent and does not present the senescence-associated secretor phenotype; however a subset of molecules are commonly altered in *in vivo* aged stroma ad *in vitro* senescence.

It is plausible that both the alteration in the collagenous stroma and the infiltration of inflammatory cells are likely to be acting in concert with one another to produce fundamental changes in both the prostate epithelial and stromal cells that can lead to prostate tumorigenesis and progression. We propose that these changes contribute in a coordinated way to induce and/or sustain prostate tumorigenesis- on one hand by altering the extracellular matrix and, on

the other, signaling through the NK-kB pathway for immune infiltration. All together, these findings provide clues to molecular events that may be related to alterations in prostate function and implicated in the high incidence of prostate cancer in the aged population.

REFERENCES:

1. Vercelli M, Quaglia A, Marani E, Parodi S: Prostate cancer incidence and mortality trends among elderly and adult Europeans. Crit Rev Oncol Hematol 2000, 35:133-144
2. Reyes I, Reyes N, Iatropoulos M, Mittelman A, Geliebter J: Aging-associated changes in gene expression in the ACI rat prostate: Implications for carcinogenesis. Prostate 2005, 63:169-186
3. Lau KM, Tam NN, Thompson C, Cheng RY, Leung YK, Ho SM: Age-associated changes in histology and gene-expression profile in the rat ventral prostate. Lab Invest 2003, 83:743-757
4. Hsing AW, Tsao L, Devesa SS: International trends and patterns of prostate cancer incidence and mortality. Int J Cancer 2000, 85:60-67
5. Abate-Shen C, Banach-Petrosky WA, Sun X, Economides KD, Desai N, Gregg JP, Borowsky AD, Cardiff RD, Shen MM: Nkx3.1; Pten mutant mice develop invasive prostate adenocarcinoma and lymph node metastases. Cancer Res 2003, 63:3886-3890
6. Bavik C, Coleman I, Dean JP, Knudsen B, Plymate S, Nelson PS: The gene expression program of prostate fibroblast senescence modulates neoplastic epithelial cell proliferation through paracrine mechanisms. Cancer Res 2006, 66:794-802
7. Begley L, Monteleon C, Shah RB, Macdonald JW, Macoska JA: CXCL12 overexpression and secretion by aging fibroblasts enhance human prostate epithelial proliferation in vitro. Aging Cell 2005, 4:291-298
8. Germeyer A, Sharkey AM, Prasadajudio M, Sherwin R, Moffett A, Bieback K, Clausmeyer S, Leanne M, Popovici RM, Hess AP, Strowitzki T, von Wolff M: Paracrine effects of uterine leukocytes on gene expression of human uterine stromal fibroblasts. Mol Hum Reprod 2008
9. Kalman J, McConathy W, Araoz C, Kasa P, Lacko AG: Apolipoprotein D in the aging brain and in Alzheimer's dementia. Neurol Res 2000, 22:330-336
10. Thomas EA, Sautkulis LN, Criado JR, Games D, Sutcliffe JG: Apolipoprotein D mRNA expression is elevated in PDAPP transgenic mice. J Neurochem 2001, 79:1059-1064
11. Provost PR, Marcel YL, Milne RW, Weech PK, Rassart E: Apolipoprotein D transcription occurs specifically in nonproliferating quiescent and senescent fibroblast cultures. FEBS Lett 1991, 290:139-141
12. Do Carmo S, Seguin D, Milne R, Rassart E: Modulation of apolipoprotein D and apolipoprotein E mRNA expression by growth arrest and identification of key elements in the promoter. J Biol Chem 2002, 277:5514-5523
13. Do Carmo S, Levros LC, Jr., Rassart E: Modulation of apolipoprotein D expression and translocation under specific stress conditions. Biochim Biophys Acta 2007, 1773:954-969
14. Adler AS, Sinha S, Kawahara TL, Zhang JY, Segal E, Chang HY: Motif module map reveals enforcement of aging by continual NF-kappaB activity. Genes Dev 2007, 21:3244-3257

15. Bernard D, Gosselin K, Monte D, Vercamer C, Bouali F, Pourtier A, Vandenbunder B, Abbadie C: Involvement of Rel/nuclear factor-kappaB transcription factors in keratinocyte senescence. Cancer Res 2004, 64:472-481
16. Salminen A, Huuskonen J, Ojala J, Kauppinen A, Kaarniranta K, Suuronen T: Activation of innate immunity system during aging: NF-kB signaling is the molecular culprit of inflamm-aging. Ageing Res Rev 2008, 7:83-105
17. Haverkamp J, Charbonneau B, Ratliff TL: Prostate inflammation and its potential impact on prostate cancer: A current review. J Cell Biochem 2007
18. Krizhanovsky V, Yon M, Dickins RA, Hearn S, Simon J, Miething C, Yee H, Zender L, Lowe SW: Senescence of activated stellate cells limits liver fibrosis. Cell 2008, 134:657-667
19. Xue W, Zender L, Miething C, Dickins RA, Hernando E, Krizhanovsky V, Cordon-Cardo C, Lowe SW: Senescence and tumour clearance is triggered by p53 restoration in murine liver carcinomas. Nature 2007, 445:656-660
20. Edwards MG, Anderson RM, Yuan M, Kendziorski CM, Weindruch R, Prolla TA: Gene expression profiling of aging reveals activation of a p53-mediated transcriptional program. BMC Genomics 2007, 8:80
21. Varani J, Dame MK, Rittie L, Fligiel SE, Kang S, Fisher GJ, Voorhees JJ: Decreased collagen production in chronologically aged skin: roles of age-dependent alteration in fibroblast function and defective mechanical stimulation. Am J Pathol 2006, 168:1861-1868
22. O'Donnell MD, McGeeney KF: An alkali digestion method to expose connective tissue fibers: a scanning electron microscopy study of rat lung. J Electron Microsc Tech 1991, 19:486-490
23. Morrison C, Thornhill J, Gaffney E: The connective tissue framework in the normal prostate, BPH and prostate cancer: analysis by scanning electron microscopy after cellular digestion. Urol Res 2000, 28:304-307
24. Campos SG, Zanetoni C, Scarano WR, Vilamaior PS, Taboga SR: Age-related histopathological lesions in the Mongolian gerbil ventral prostate as a good model for studies of spontaneous hormone-related disorders. Int J Exp Pathol 2008, 89:13-24
25. Kiefer JA, Farach-Carson MC: Type I collagen-mediated proliferation of PC3 prostate carcinoma cell line: implications for enhanced growth in the bone microenvironment. Matrix Biol 2001, 20:429-437
26. Ilio KY, Nemeth JA, Sensibar JA, Lang S, Lee C: Prostatic ductal system in rats: changes in regional distribution of extracellular matrix proteins during castration-induced regression. Prostate 2000, 43:3-10
27. Provenzano PP, Eliceiri KW, Campbell JM, Inman DR, White JG, Keely PJ: Collagen reorganization at the tumor-stromal interface facilitates local invasion. BMC Med 2006, 4:38
28. Provenzano PP, Inman DR, Eliceiri KW, Knittel JG, Yan L, Rueden CT, White JG, Keely PJ: Collagen density promotes mammary tumor initiation and progression. BMC Med 2008, 6:11
29. Krtolica A, Parrinello S, Lockett S, Desprez PY, Campisi J: Senescent fibroblasts promote epithelial cell growth and tumorigenesis: a link between cancer and aging. Proc Natl Acad Sci U S A 2001, 98:12072-12077

30. Coppe JP, Patil CK, Rodier F, Sun Y, Munoz DP, Goldstein J, Nelson PS, Desprez PY, Campisi J: Senescence-Associated Secretory Phenotypes Reveal Cell-Nonautonomous Functions of Oncogenic RAS and the p53 Tumor Suppressor. PLoS Biol 2008, 6:e301
31. Jeyapalan JC, Ferreira M, Sedivy JM, Herbig U: Accumulation of senescent cells in mitotic tissue of aging primates. Mech Ageing Dev 2007, 128:36-44
32. Jeyapalan JC, Sedivy JM: Cellular senescence and organismal aging. Mech Ageing Dev 2008, 129:467-474
33. Herbig U, Ferreira M, Condel L, Carey D, Sedivy JM: Cellular senescence in aging primates. Science 2006, 311:1257
34. Krishnamurthy J, Torrice C, Ramsey MR, Kovalev GI, Al-Regaiey K, Su L, Sharpless NE: Ink4a/Arf expression is a biomarker of aging. J Clin Invest 2004, 114:1299-1307
35. Arnesen SM, Lawson MA: Age-related changes in focal adhesions lead to altered cell behavior in tendon fibroblasts. Mech Ageing Dev 2006, 127:726-732

SUPPORTING DATA:

Table 1. Gene expression changes in the mouse prostate stroma from young (4 months) and old (24 months) C57Bl/6 mice

Symbol	Gene name	Fold Change (Old/Young)	GO Function
Ralyl	RALY RNA binding protein-like	+36	nucleic acid binding
Serpinb5	serine (or cysteine) peptidase inhibitor, clade	+9	serine-type endopeptidase inhibitor activity
Trp63	transformation related protein 63	+7.2	transcription factor activity
2010016I18Rik	RIKEN cDNA 2010016I18 gene	+7	
Slc26a3	solute carrier family 26, member 3	+6.9	anion exchanger activity; sulfate porter activity
BC020489	cDNA sequence BC020489	+6.5	
LOC432593	Hypothetical gene supported by AK078606	+6.1	
5330417C22Rik	RIKEN cDNA 5330417C22 gene	+6.1	
C130026I21Rik	RIKEN cNDA C130026I21 gene	+4.6	
Ccl8	chemokine (C-C motif) ligand 8	+4.6	chemokine activity; heparin binding
A530040E14Rik	RIKEN cDNA A530040E14 gene	+4.2	
Gbp4	macrophage activation 2	+4.2	GTP binding;GTPase activity
Il7r	interleukin 7 receptor	+4	antigen binding;interleukin-7 receptor activity
Gyltl1b	glycosyltransferase-like 1B	+3.9	transferase activity\, transferring hexosyl groups
Krt15	keratin 15	+3.8	structural constituent of cytoskeleton
Cd8a	CD8 antigen, alpha chain	+3.8	
Fmo3	flavin containing monooxygenase 3	+3.7	dimethylaniline monooxygenase (N-oxide-forming) activity;disulfide oxidoreductase activity
Pkp1	plakophilin 1	+3.1	cell adhesion molecule activity;intermediate filament binding;structural constituent of epidermis
Ccl5	chemokine (C-C motif) ligand 5	+3	chemokine activity
Rnmt	RNA (guanine-7-) methyltransferase	+2.9	RNA binding;mRNA (guanine-N7-)-methyltransferase activity
Zfp26	zinc finger protein 26	+2.7	
KIAA0746	KIAA0746 protein	+2.6	
Cd8b1	CD8 antigen, beta chain 1	+2.6	MHC class I protein binding;MHC class I receptor activity;coreceptor activity;protein binding
Ccl7	chemokine (C-C motif) ligand 7	+2.4	chemokine activity;heparin binding
B930041F14Rik	RIKEN cDNA B930041F14 gene	+2.4	
Apod	apolipoprotein D	+2.3	high-density lipoprotein binding;lipid binding;lipid transporter activity
Olfr971	olfactory receptor 971	+2.3	
Grhl1	grainyhead-like 1 (Drosophila)	+2.2	
Tcrb-V13	T-cell receptor beta, variable 13	+2.2	
Itgal	integrin alpha L	+2.2	cell adhesion receptor activity;magnesium ion binding
Oasl1	2'-5' oligoadenylate synthetase-like 1	+2	ATP binding;RNA binding;nucleotidyltransferase activity
Tsku	leucine rich repeat containing 54	+2	
Hlcs	holocarboxylase synthetase (biotin-	+2	biotin-[acetyl-CoA-carboxylase] ligase activity;biotin-[methylcrotonoyl-CoA-carboxylase] ligase
Inadl	InaD-like (Drosophila)	+2	ATP binding;protein binding;structural constituent of ribosome
Tcl1b2	T-cell leukemia/lymphoma 1B, 2	+2	
Cds2	CDP-diacylglycerol synthase (phosphatidate	+1.9	phosphatidate cytidylyltransferase activity
Car1	carbonic anhydrase 1	+1.9	carbonate dehydratase activity;zinc ion binding
Clcc1	chloride channel CLIC-like 1	+1.9	
Atp11a	ATPase, class VI, type 11A	+1.9	ATP binding;magnesium ion binding;phospholipid-translocating ATPase activity
Vgll3	RIKEN cDNA 1700110N18 gene	+1.9	
Rorc	RAR-related orphan receptor gamma	+1.8	steroid hormone receptor activity;transcription factor activity
Efhd1	EF hand domain containing 1	+1.8	calcium ion binding
H2-Q1	histocompatibility 2, Q region locus 1	+1.8	
Fhl3	four and a half LIM domains 3	+1.7	actin binding
Pak3	p21 (CDKN1A)-activated kinase 3	+1.7	ATP binding;protein serine/threonine kinase activity;protein-tyrosine kinase activity
Wdr45l	Wdr45 like	+1.7	acid phosphatase activity;molecular_function unknown
Perp	PERP, TP53 apoptosis effector	+1.7	structural constituent of eye lens
Snx26	sorting nexin 26	+1.7	GTPase activator activity;protein transporter activity
Sectm1b	secreted and transmembrane 1	+1.6	
LOC628746	Similar to RING1 and YY1 binding protein	+1.6	
Tex10	testis expressed gene 10	+1.6	
BC050196	cDNA sequence BC050196	+1.6	
Cd24a	CD24a antigen	+1.5	
Tmco4	transmembrane and coiled-coil domains 4	+1.5	catalytic activity
Rab3d	RAB3D, member RAS oncogene family	+1.5	GTP binding;RAB small monomeric GTPase activity;protein transporter activity
Olfr788	olfactory receptor 788	+1.5	
Olfr1131	olfactory receptor 1131	+1.5	
Rassf7	Ras association (RalGDS/AF-6) domain	+1.4	methylated-DNA-[protein]-cysteine S-methyltransferase activity
Csf2rb1	colony stimulating factor 2 receptor, beta 1,	+1.3	hematopoietin/interferon-class (D200-domain) cytokine receptor activity
Ccdc106	coiled-coil domain containing 106	-2.37	
Ccnd2	cyclin D2	-1.84	
Mest	mesoderm specific transcript	-2.19	epoxide hydrolase activity
Grik4	glutamate receptor, ionotropic, kainate 4	-2.71	glutamate-gated ion channel activity;kainate selective glutamate receptor activity;potassium

Fold change values are averages of the anterior and dorsal prostate measurements in the Agilent microarray analysis. Positive values indicate an increase, and negative values indicate a decrease in gene expression in the old prostate. Gene names in italics have been verified by quantitative real-time PCR. Gene names in bold appear to be novel and not previously reported to be altered with *in vivo* aging or *in vitro* senescence.

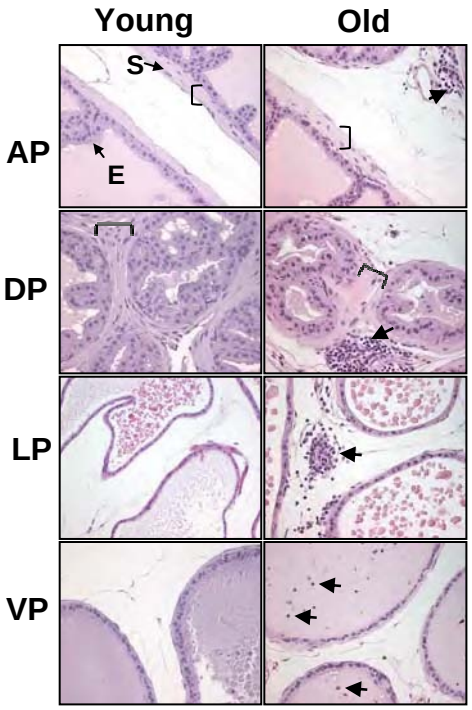

Figure 1. Histological features of prostates from young and old mice as observed in 4-µm hematoxylin and eosin-stained sections from formalin-fixed tissue. E: Luminal epithelium; S: Stroma adjacent to the epithelial cells. Thick adjacent cellular stroma observed in dorsal and anterior lobe (brace). H& E revealed frequent areas of inflammatory cell infiltration in the prostates of old animals (arrow). AP: Anterior prostate; DP: dorsal prostate; LP: lateral prostate and VP: ventral prostate. (Magnification: x20).

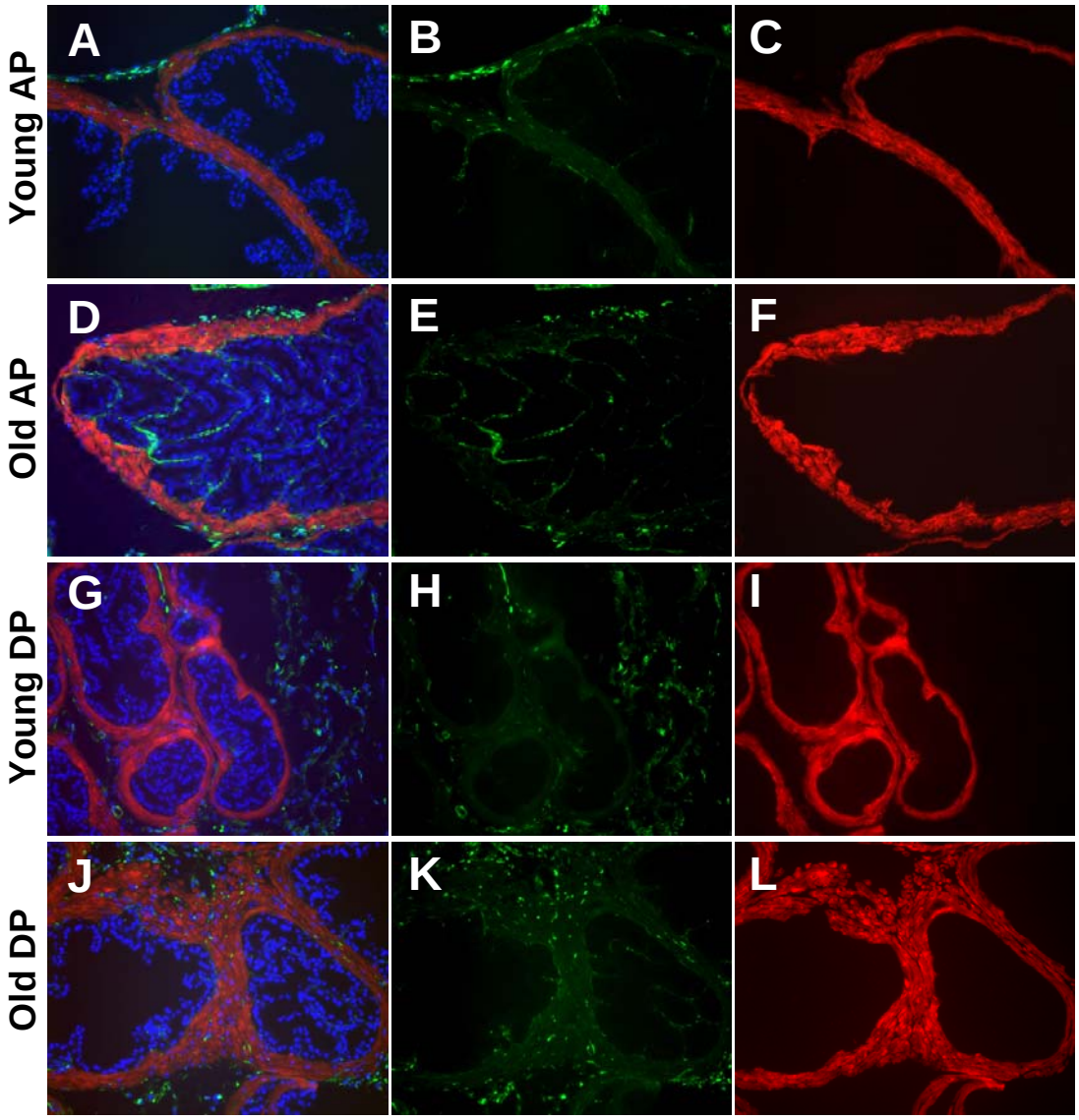

Figure 2. Double immunofluorescent stain for smooth-muscle-actin (Red; C,F,I and L) and vimentin (green, B, E, H and K). A, D, G and J merge images (Blue: DAPI, Red: SM-Actin, Green: Vimentin). DP: Dorsal Prostate

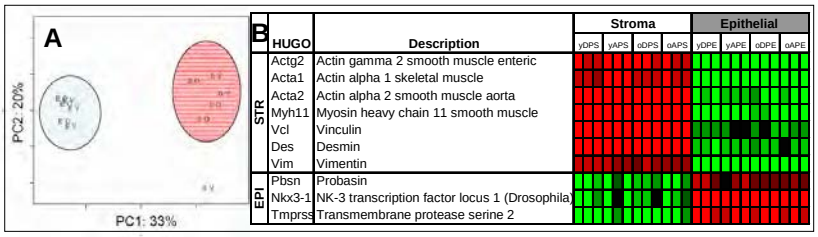

Figure 3. Laser capture microdissected stroma and epithelium: Sample purity. A) Principal Component Analysis for dorsal prostate stroma and epithelial microdissected samples from young and old animals. EO: old epithelium; EY: young epithelium; SO: old stroma; SY: young stroma. B) Transcript abundance levels (Log 2 ratios) obtained from MPEDB arrays of known stromal and epithelial markers in LCM samples acquired from mouse prostate stroma and epithelium.

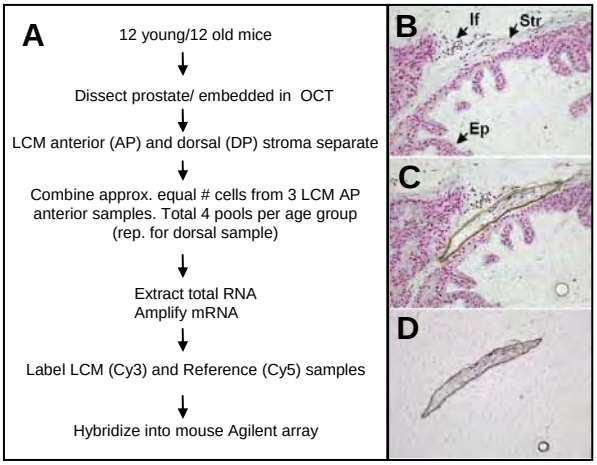

Figure 4. A) Experimental design. Prostates from 12 young (4 months-old) and 12 old (24 months-old) C57BL/6 mice were resected and immediately frozen in OCT. Laser capture microdissection was performed in the cellular adjacent stroma. Each experimental sample represents a pool of approximately equal number of cells (as calculated by the microdissected area) for the dorsal and anterior prostatic lobes from four animals. Eight independent experimental samples were created per age group for a total of sixteen samples (eight microarray experiments per age group): (4 young and 4 old anterior prostate stroma and 4 young and 4 old dorsal prostate stroma). Amplified RNA from each experimental sample was hybridized against a reference pool (mouse gold standard) onto an Agilent customized mouse cDNA array using Cy3 dye to label the experimental samples and Cy5 dye for the reference sample. B-D) Images of mouse dorsal prostate tissue sections (7uM) during the LCM procedure. B) Pre-Capture image shows stroma and epithelium (pink) with a focal area of inflammatory cells (if) which was avoided during capturing. C) captured stromal cells D) Stromal cells isolated on the LCM cap.

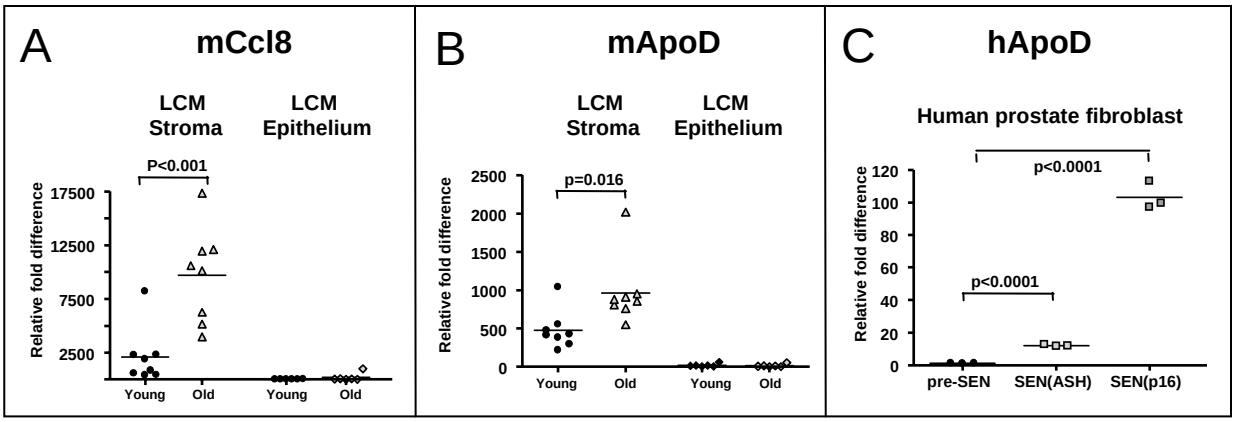

Figure 5. Analysis of age-related changes in genes expression in the aged prostate by qRT-PCR. RNAs were reverse transcribed and amplified using qRT-PCR with primers specific for Ccl8 and ApoD. RNAs used were as follow: microdissected stroma and epithelium from dorsal (n=4) and anterior (n=4) lobes used in microarray analyses (LCM stroma and LCM epithelium); and human prostate fibroblast. A) Measurement of Ccl8 from RNA isolated from laser captured stroma and epithelium from young (n=8 4-months of age) and old (n=8; 24-months of age) mice. B) Measurement of ApoD transcript levels from RNA isolated from laser captured stroma and epithelium from young (n=8 4-months of age) and old (n=8; 24-months of age) mice. C) Measurement of human APOD transcript levels from RNA isolated from human pre- and senescent prostate fibroblast. Pre-SEN: pre-senescent cells; SEN(ASH) cell induced to senesce by H_2O_2; SEN(p16) cell induced to senesce by over-expressing p16. YWHAZ expression levels were used to normalize the human qRT-PCR data. Ribosomal protein S16 expression levels were used to normalize mouse qRT-PCR data. Normalized results are expressed relative to the lowest expressing value.

Figure 6. Gene expression comparison between prostatic microdissected adjacent stroma (**STR**), prostatic microdissected epithelial cells (**EPI**) and white blood cells (**WBC**). Gene expression levels are shown as Log2 Ratios against a common mouse gold standard. Shown are the 63 genes most differentially expressed between young and old microdissected stroma according to SAM analysis (FDR<10%). Red: genes highly expressed in the experimental samples compared to the mouse gold standard. Green: genes with low expression in the experimental samples compared to the mouse gold standard.

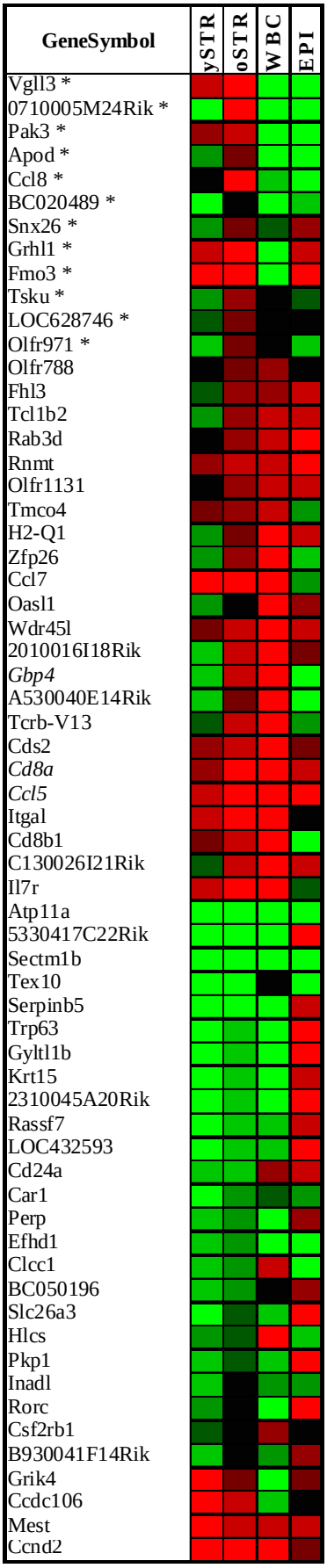

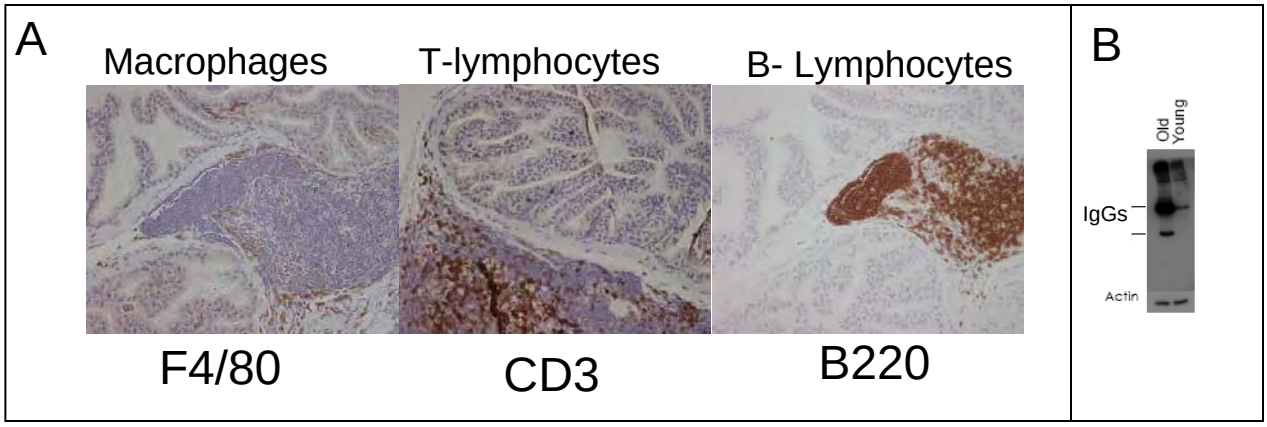

Figure 7. **A)** Immunohistochemical analysis of 4uM paraffin sections from anterior prostate of 24-months-old mice. Sections were stained with anti-CD3, anti-B220 and anti-F4/80, which recognize T-cell, B-cells and macrophages respectively. IHC demonstrated a high number of inflammatory cells within the aged prostate tissue. **B)** Western Blot analysis of mouse prostate tissue extracts from old (24 months-old) and young (4 months-old) animals. Blot was probe with anti-mouse secondary antibody. Same blot was probed with an antibody against actin for loading control.

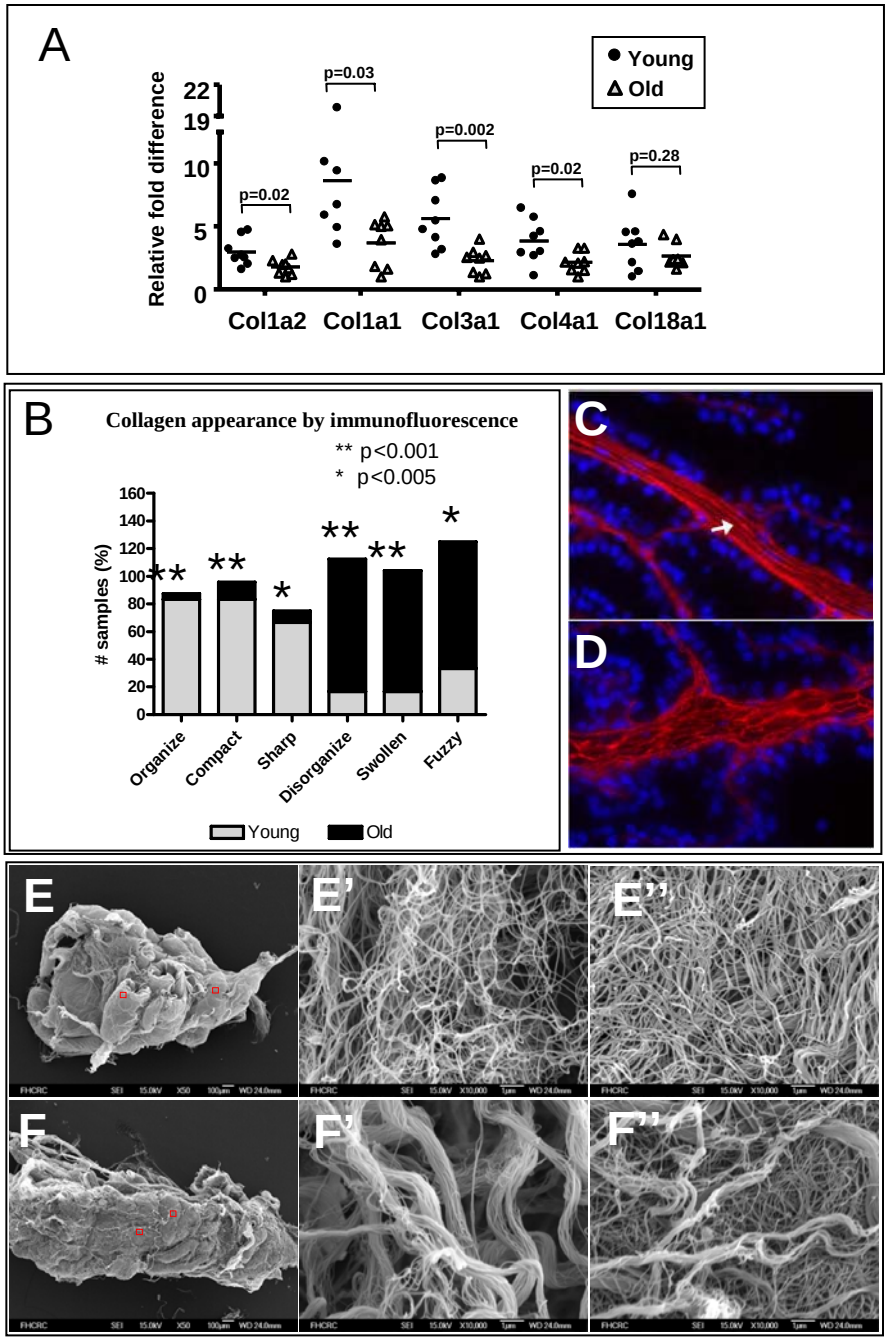

Figure 8. Collagen alterations. A) qRT-PCR for Col1a2, Col1a1,Col3a1, Col4a1 and Col18a1 from RNA isolated from laser captured stroma from young (n=8 4-months of age) and old (n=8; 24-months of age) anterior prostate. Ribosomal protein S16 expression levels were used to normalize qRT-PCR data. Normalized results are expressed relative to the lowest expressing value for each gene tested. B) Qualitative and Quantitative confocal analysis for the appearance of collagen fibers from young (n=3; 4 images per mouse) and old (n=3; 4 images per mouse) from Collagen Type I immunofluorescent images. C,D) Collagen Type I immunofluorescent staining of frozen sections from anterior prostate lobes from 4- (C) and 24-months (D) of age mice (Magnification: x40). Note the coarse appearance and less regular distribution of collagen fibers in old prostates compared to the fine collagen fibers and highly organized network in the young prostate. E) Scanning Electron Microscopy of acellular preparationS from young and old anterior prostate.

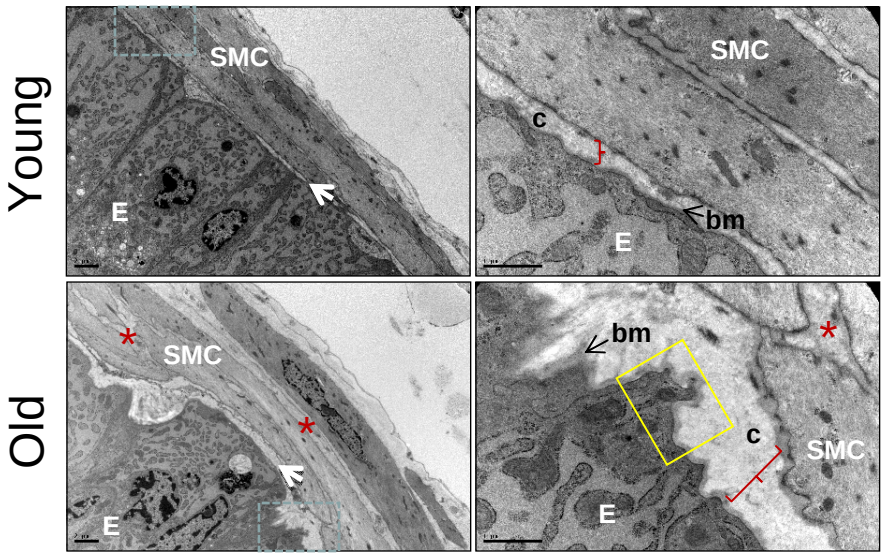

Figure 9. Transmission electron microscopy of cross sections from young (A,C) and old (B,D) normal mouse prostate. E indicates luminal epithelial; SMC, smooth muscle cells; bm and white arrow: basement membrane; c: collagen fibrils; Brace: collagenous layer underneath the basement membrane, asterisk: space between SMC. Yellow square: epithelial cytoplasmic projections.

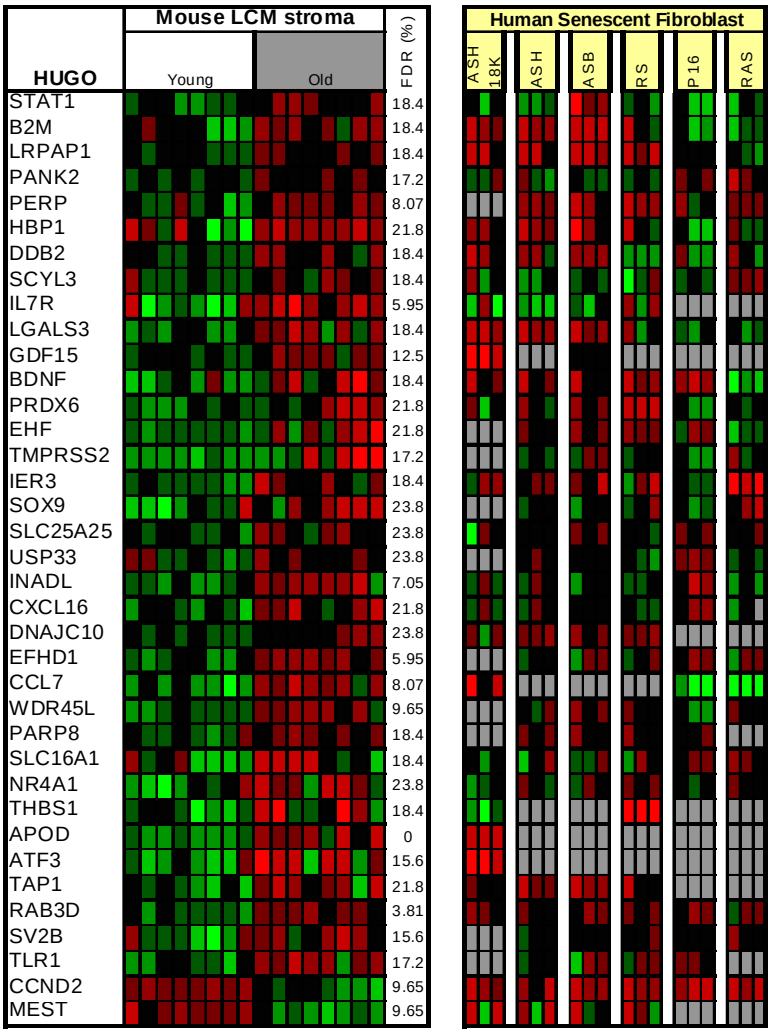

Figure 10. Heat map of age related changes in the prostate stroma compared to Human *in vitro* senescence . The heat map represent the significantly differentially expressed genes from *in vivo* aged stroma (less than 25% FDR) that overlap with significantly altered genes (FDR <25%) in at least one human senescent data set. Red indicates increased expression; green indicates decreased expression; black represents no change in expression and grey represents no information on that gene.